The Journal of Experimental Biology 203, 2565–2579 (2000)
Printed in Great Britain © The Company of Biologists Limited 2000
JEB2652

LOCOMOTOR REPERTOIRE OF THE LARVAL ZEBRAFISH: SWIMMING, TURNING AND PREY CAPTURE

SETH A. BUDICK AND DONALD M. O'MALLEY*

Department of Biology, 414 Mugar Hall, Northeastern University, Boston, MA 02115, USA

*e-mail: domalle@lynx.neu.edu

Accepted 7 June; published on WWW 9 August 2000

Summary

Larval zebrafish (*Brachydanio rerio*) are a popular model system because of their genetic attributes, transparency and relative simplicity. They have approximately 200 neurons that project from the brainstem into the spinal cord. Many of these neurons can be individually identified and laser-ablated in intact larvae. This should facilitate cellular-level characterization of the descending control of larval behavior patterns. Towards this end, we attempt to describe the range of locomotor behavior patterns exhibited by zebrafish larvae. Using high-speed digital imaging, a variety of swimming and turning behaviors were analyzed in 6- to 9-day-old larval fish. Swimming episodes appeared to fall into two categories, with the point of maximal bending of the larva's body occurring either near the mid-body (burst swims) or closer to the tail (slow swims). Burst swims also involved larger-amplitude bending, faster speeds and greater yaw than slow swims. Turning behaviors clearly fell into two distinct categories: fast, large-angle escape turns characteristic of escape responses, and much slower routine turns lacking the large counterbend that often accompanies escape turns. Prey-capture behaviors were also recorded. They were made up of simpler locomotor components that appeared to be similar to routine turns and slow swims. The different behaviors observed were analyzed with regard to possible underlying neural control systems. Our analysis suggests the existence of discrete sets of controlling neurons and helps to explain the need for the roughly 200 spinal-projecting nerve cells in the brainstem of the larval zebrafish.

Key words: locomotion, swimming, zebrafish, *Brachydanio rerio*, kinematics, prey capture, neuron.

Introduction

The descending control of locomotor behaviors is an area of neurobiology with many unanswered questions. In the case of mammals, the millions of descending fibers that project into the spinal cord, together with their numerous origins, pose a considerable problem. Understanding just one subset of these descending neurons, for example the reticulospinal neurons, is difficult because of the variety of reticulospinal cell types and their intermingling with other cell types in the brainstem (Brodal, 1981; Siegel and Tomaszewski, 1983). This problem is reduced in scope in fishes because of the reduced numbers of nerve cells and nuclei that project to the spinal cord, but even in these simpler systems we do not have a cellular-level understanding of the neural control systems. A recent technical advance in this area has been the use of fluorescent Ca^{2+} indicators to label larval zebrafish neurons retrogradely. This permits optical recording of neural/Ca^{2+} activity in the spinal cord (Fetcho and O'Malley, 1995) and brainstem (O'Malley et al., 1996) of intact larval zebrafish. This same technique facilitates the laser-ablation of specific neurons, after which behavioral deficits can be quantified using high-speed behavioral recordings (Fetcho and Liu, 1999). In addition to its transparency, the larval zebrafish (*Brachydanio rerio*) is relatively simple (for a vertebrate animal), and many of the neurons that project from the brain into the spinal cord can be individually identified, both in histological preparations (Metcalfe et al., 1986; Bernhardt et al., 1990; Eisen, 1999) and *in vivo*, using confocal microscopy (Fetcho and O'Malley, 1997; Fetcho et al., 1998). These optical approaches have recently been applied to studies of the escape behavior.

The Mauthner cell is a command neuron that, in teleost fish, triggers an escape response each time it fires an action potential (Zottoli, 1977; Kimmel et al., 1980; Eaton et al., 1981; Faber et al., 1989). The involvement of two other reticulospinal neurons in the escape behavior (cells MiD2cm and MiD3cm) was first suggested on the basis of their anatomical similarity to the Mauthner cell (Metcalfe et al., 1986). This anatomical similarity, together with quantitative electromyographic and kinematic analyses, led to the proposal that these cells provide directional control of the escape response (Foreman and Eaton, 1993). Optical recordings of the neural activity of these cells during escape responses (O'Malley et al., 1996) and subsequent laser-ablation experiments (Liu and Fetcho, 1999) confirmed the hypothesis of Foreman and Eaton (1993) and demonstrated that these neurons play a controlling role in this

behavior. Of particular significance is that these studies provided direct evidence that serially homologous neurons in successive hindbrain segments (i.e. the Mauthner cell, MiD2cm and MiD3cm) contribute to a common behavior, the escape response. Six other sets of potential segmental homologues were also described by Metcalfe et al. (1986). This may, therefore, be a general means by which brainstem neurons are functionally organized, especially since the hindbrain is relatively well-conserved across vertebrate species (Fraser et al., 1990; Guthrie, 1995; Bass and Baker, 1997).

Young larval zebrafish (less then 7 days old) appear to have approximately 200 neurons that project from the brain into the spinal cord. These include roughly 100 reticulospinal neurons, approximately 30 IC (ipsilateral caudal) neurons, and approximately 20 each of T-reticular neurons, vestibulospinal neurons and nucleus medial longitudinal fasciculus (MLF) neurons (Metcalfe et al., 1986; Kimmel et al., 1985; E. Gahtan, personal communication). Apart from the three specific pairs of neurons discussed above, the precise functional role of the remainder of these 200 or so neurons is not known. But descending locomotor control signals must be sent to the spinal cord either through these neurons or perhaps through other as yet unidentified descending neurons. Because the total number of neurons appears to be relatively small, functionally significant numbers of them (in principle, any desired subset) can be specifically targeted and laser-ablated. It should be possible, therefore, to optically dissect the larva's descending control system to elucidate the cellular control of swimming, turning and other locomotor behaviors. Because these same neurons are present and identifiable in both adult zebrafish (Lee and Eaton, 1991) and adult goldfish (*Carassius auratus*) (Lee et al., 1993), they may form the core of an adult teleost locomotor control system (Prasada Rao et al., 1987).

Fishes, as a group, exhibit a great diversity of swimming styles (Wardle et al., 1995; Van Raamsdonk et al., 1998). Single species can exhibit a variety of swimming patterns, as occurs in bluegill sunfish (*Lepomis macrochirus*) in which three distinct patterns were observed at successively greater swimming speeds (Jayne and Lauder, 1994). Because of their small size, larval swimming has not been examined in as great detail. The early development of motor behaviors has recently been characterized in zebrafish embryos (Saint-Amant and Drapeau, 1998). In several larval fishes, including plaice (*Pleuronectes platessa*), herring (*Clupea harengus*) and chinook salmon (*Oncorhynchus tshawytscha*), detailed kinematics have been reported for burst swimming (Batty and Blaxter, 1992; Hale, 1996). In larval and juvenile zebrafish, ontogenetic changes in swimming speed and acceleration have been reported along with duration and distance covered during bouts of routine swimming (Fuiman and Webb, 1988), while a more recent study characterized hydrodynamic flow patterns around larval and adult zebrafish (Müller et al., 2000). In no case, however, has a larval fish at a particular developmental stage been reported to exhibit several distinct patterns of swimming analogous to those observed in adult fish.

Less is known about turning behavior in fishes. While escape-related turning behaviors have been studied extensively (see, for example, Kimmel et al., 1974; Foreman and Eaton, 1993), and kinematic data are available on the S-starts used in predation (Domenici and Blake, 1997; Spierts and Van Leeuwen, 1999), other more 'routine' turning behaviors used in navigation, foraging or related behaviors have been less studied (McClellan and Hagevik, 1997). Fuiman and Webb (1988) reported that in zebrafish larvae the proportion of swimming bouts that begin with large-angle turns increases with the length of the larva, but the frame rate of the video recordings used at that time limited the kinematic analyses that could be performed. Regarding prey capture by larval zebrafish, there are, to our knowledge, no published high-speed kinematic studies, although prey capture by other larval fish has been shown to involve both ram- and suction-feeding strategies (Drost and Van den Boogaart, 1986; Coughlin, 1994).

Zebrafish have attracted intense interest as a model vertebrate organism, and many central nervous system and behavioral mutants have recently been generated (see, for example, Brockerhoff et al., 1995; Nicolson et al., 1998). Our objective was to generate a catalogue of larval zebrafish locomotor behaviors using high-speed digital imaging. While high-speed imaging is known to be essential for examining fast behaviors such as the escape response (Eaton et al., 1977; Harper and Blake, 1989), precise kinematic analysis of even the slower swimming and turning behaviors described here required high-speed imaging. Our specific goal in describing the locomotor repertoire was to establish the range of behaviors in which deficits might ultimately be produced by laser-ablation experiments. We report here variations in swimming and turning behaviors that have implications for the neural control of locomotion.

Materials and methods

Animals

Fertilized eggs were collected from a breeding laboratory population of zebrafish (*Brachydanio rerio*), transferred to 10% Hanks' solution and maintained at approximately 25 °C (Westerfield, 1995). After hatching, the larvae were kept under the same conditions for the duration of the study. Maintaining zygotes and larvae at this relatively low temperature slightly retards both their rate of growth and depletion of the larval yolk sac. This allows a somewhat longer period to study locomotor behaviors before feeding the larvae becomes necessary. Larvae were not fed prior to the evaluation of locomotor or feeding behaviors. Behavioral observations were performed on fish between 6 and 9 days post-fertilization. Unfed larvae continue to grow during this period: the mean total length of the fish at 6 days post-fertilization was 3.68±0.14 mm (N=8), while 9-day-old fish measured 3.93±0.13 mm (means ± S.E.M., N=8).

Experimental protocols

To observe swimming and turning behaviors, larvae were individually transferred to small plastic Petri dish lids (4 cm diameter) containing 10% Hanks' solution. To observe

feeding, larvae were transferred into dish lids containing a suspension of *Paramecium aurelia*. These dishes were filled to a depth of approximately 2 mm. To avoid accidental breakage of the glass micropipettes used to elicit escapes, the bottom of the dish was coated with a thin layer of agar. Larval behavior was captured with a high-speed, MD4256 digital camera (EG&G Reticon, Sunnyvale, CA, USA) attached to a dissecting microscope running on a Pentium PC. Most data were collected at 500 frames s^{-1}. Some escape behaviors were imaged at 1000 frames s^{-1}, although the images shown were collected at 500 frames s^{-1}. The larvae were acclimated to the bright lights necessary for high-speed recording for at least 3 min prior to observation. All experiments were conducted at ambient room temperature, usually 25–26 °C, but, because of evaporative cooling, the temperature of the water in the dish was approximately 22 °C. The fiber-optic lights (Fiber-Lite, Dolan-Jenner, Lawrence, MA, USA) used during the recording sessions raised the dish temperature slightly, to between 22 and 23 °C. Unprocessed, digital movies of the different behaviors can be viewed at www.omalleylab.neu.edu.

Recording of routine turns and swimming bouts

After acclimation to the testing dish, fish were observed until they spontaneously performed either a routine turn or a swimming behavior, at which point the images in the camera's frame buffer were saved to disk. A routine turn was defined operationally as a spontaneous bend, i.e. a bend in response to no apparent stimulus, that resulted in a change in heading of at least 30 °, as measured at the completion of the first bend. This criterion was chosen to distinguish routine turns from swimming bouts, which often begin with small, transient direction changes that produce little, if any, sustained change in heading; we did not want to include forward swimming bouts in our analysis of routine turns. Swimming was defined operationally as three or more spontaneous, consecutive cycles of bending that did not involve noticeable changes in direction. A single swimming episode and multiple turns were recorded from each fish. The direction change was measured for all recorded turns. For the measurement of angular velocity, bend duration and counterbend angle, only one turn per fish was analyzed.

Recording of escape turns

After acclimation and during a period of relative quiescence, a glass micropipette (approximately 50 μm tip diameter) connected to a picospritzer (Parker Hannifin, Fairfield, NJ, USA) was slowly moved to within approximately 0.5 mm of the larva using a micromanipulator. The micropipette tip was dyed red to make it easier to position. A brief pulse of water (3–5 ms) was directed at either the head or tail of the larva. Head-directed stimuli were aimed at the ear, while tail-directed ones were aimed approximately half-way between the anal pore and the tip of the tail. With each larva, a low-intensity stimulus, i.e. a 3 ms pulse of water at a gauge pressure of 30 psi (207 kPa), was initially used in an attempt to elicit an escape response. If the larva failed to respond, the stimulus strength was gradually increased until a response occurred. The maximum stimulus intensity used was a 5 ms pulse at a pressure of 50 psi (345 kPa), but most fish responded at lower intensities. One or more escapes were elicited from an individual larva. We alternated between head- and tail-directed stimuli and between stimuli originating on the left and right sides of the fish. An interval of at least 2 min and at most 5 min passed between trials.

Feeding observations

The larvae were observed feeding in a protozoan medium suspension containing approximately 1000 *Paramecium* ml^{-1}. In all images shown of prey capture, the *Paramecium* were digitally highlighted to enhance their contrast with the background. Because of their motion, *Paramecium* are quite evident during moderately fast playback of capture sequences (see web site), and their location is certain, even though they appear faint in uncorrected still images. After being placed in the Petri dish lid, larvae were observed until they fed upon one or more *Paramecium*.

Image analysis

Preliminary analysis of the behavioral recordings was performed with the Reticon MD4256 software, which allowed variable-speed playback of the previously recorded behaviors. We first identified swimming and turning episodes that met the criteria described above, i.e. three or more cycles of swimming or spontaneous turns of 30 ° or more. Detailed manual measurements of these behaviors were performed on individual frames taken from the behavioral episodes. These measurements were made on printed copies whose brightness and contrast had been digitally adjusted on a Power Macintosh G3 to improve visualization of the larvae (Adobe PhotoShop, San Jose, CA, USA). Feeding episodes were not analyzed quantitatively.

Variables used for analysis of escape turns, routine turns and swimming

The following variables of escape and routine turns were manually measured. (i) Direction change: the change in heading of the fish from its starting position to its heading at the completion of the initial bend. The heading was determined by drawing a line from the midline of the anterior end of the swimbladder to the midline of the tip of the snout. The completion of the bend was the time point at which the change in heading reached its maximum, before stopping and reversing direction. (ii) Time point of maximal bending. For the initial bend, the time point when the bend is completed corresponds fairly well to the point at which the bending of the larval zebrafish is 'maximal'. We are referring here specifically to the time point at which the greatest length of the body is substantially bent, rather then later time points when a portion of the tail might be strongly curved, but the forward half of the body is fairly straight. While the 'heading-change' approach was useful for identifying this time point during the first bend in a sequence (e.g. frame 9 in Fig. 2 and frame 8 in Fig. 4), it

was not useful for subsequent bends because the heading changes were often very slight. A time point that better captured the 'point of maximal bending' of interest in these subsequent bends was the frame in which a caudally traveling wave of bending caused the very tip of the fish's tail to 'flip direction', i.e. to turn towards the side of the new bend. In Fig. 4, for example, this happens between frames 13 (asterisk) and 14, and so frame 14 would be considered the time point of maximal bending for the second bend. While more complex procedures might be used to define a point of 'maximal' bending, our procedure provided a straightforward means of capturing a time point when the bending was quite substantial, and facilitated a comparison of the degree of bending during different behaviors. (iii) Head–tail angle: the angle formed between the head and tail of the fish at the time point of maximal bending. First, a line was drawn along the midline of the fish, generating a curve that defined the bending of the fish (Fig. 1). Next, a line was drawn at a tangent to the most rostral portion of this curve. This line is oriented to the *x*-axis in Fig. 1. A second line was drawn at a tangent to the midline at the most caudal portion of the bend. The angle between this line and the *x*-axis is the head–tail angle. Construction of this angle is illustrated for representative large and small bends. (iv) Bend amplitude. Subtracting the head–tail angle from 180 ° (i.e. the head–tail 'angle' when the fish is straight) yields the bend amplitude, a measure (in degrees) of the magnitude of the bend. Note that in the largest escapes, where the head direction 'crosses' the tail direction, the head–tail angle becomes negative and can result in bend amplitudes greater than 180 °. (v) Bend duration. The time between initiation of the turn and point of maximal bending. (vi) Angular velocity. Dividing the amplitude of the initial bend by the duration of that bend yields the angular velocity. (vii) Counterbend angle is the amplitude of the second bend of an escape or routine turn. Differences between escape and routine turns for the kinematic variables analyzed were tested using two-tailed, heteroscedastic *t*-tests.

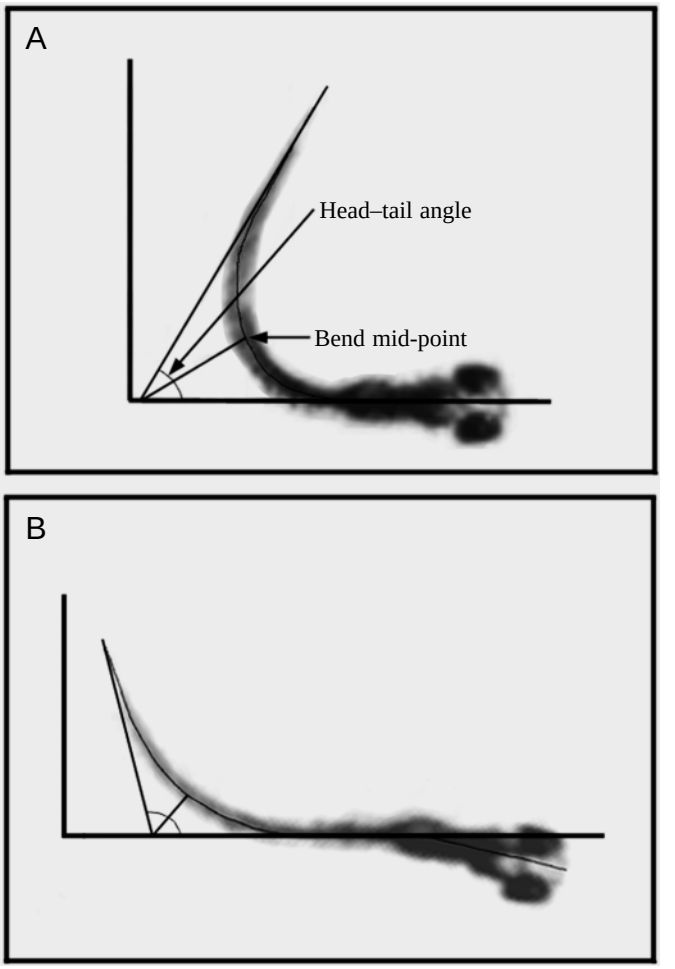

Fig. 1. Determination of head–tail angle and bend location. Examples are shown for representative frames from a burst swim (A) and a slow swim (B). In both cases, a line is drawn at a tangent to the most caudal and the most rostral portion of the 'bend', i.e. the curve running through the midline of the animal. The angle between these lines is the head–tail angle. The intersection between the shortest line from the vertex of this angle and the midline of the fish is defined as the midpoint of the bend. The 'bend location' is the distance from the tip of the snout to the midpoint of the bend. 'Bend location' is not a standard kinematic variable, but rather reflects distinct visual differences between the two swimming categories.

Swimming-specific variables

The following five variables were measured manually in swimming episodes. (i) Bend location: the site along the rostral–caudal axis that forms the midpoint of the bend. The shortest possible line is drawn between the vertex of the head–tail angle and the midline of the fish (Fig. 1). This line intersects with the midpoint of the bend. The distance from the rostral end of the fish to this point, expressed in total body lengths, is the bend location. (ii) Mean bend amplitude: the average amplitude of all bends in a bout of swimming. (iii) Yaw: the maximum discrepancy, during each half of the swimming cycle, between the direction in which the head is pointing and the direction of travel of the larva's center of mass. The Cartesian coordinates of a fixed point on the fish just rostral to the swimbladder, which approximates the center of mass, were recorded during the moment of maximum bend amplitude of each bend in a swimming bout using Graphic Converter software (Lemke Software, Peine, Germany). The least-squares regression on the coordinates of these points yielded the mean direction of travel. The mean yaw was the average of the yaw values measured over all half-cycles of swimming included in the swimming bout. (iv) Swimming speed was calculated by dividing the distance traveled by the larva's center of mass during a swimming bout by the duration of the bout. (v) Tail-beat frequency. The reciprocal of the duration of a tail-beat cycle is the tail-beat frequency for that cycle. The tail-beat cycle is the time required for one complete cycle of bending of the larvae's right and left sides. The tail-beat frequency for a bout of swimming (see below) was the average of the tail-beat frequencies for all swimming cycles within that bout. Differences between burst and slow swims

for the kinematic variables analyzed were tested using two-tailed, heteroscedastic *t*-tests.

To be considered for analysis, a swimming bout had to contain a minimum of three complete tail-beat cycles. As will be discussed in the Results, swimming was divided into two classes, slow and burst swims, on the basis of bend location. Because burst swims typically make a transition into a slow swimming pattern before the fish comes to a halt, single swimming episodes often contained bends that fell within both categories of swimming. In all cases, only those portions of swimming episodes that contained at least three consecutive tail-beat cycles, made up exclusively of either slow or burst swimming, were defined as a bout and analyzed. Other portions of such swimming episodes were not analyzed.

Results

Turning behavior

We first examined turning behaviors. The first type of turn, a spontaneous slow-speed turn, which we refer to as a 'routine' turn, is shown in a series of images displayed at 4 ms intervals in Fig. 2 (images were collected at 2 ms intervals, but only every other image is shown). In such turns, the fish makes a bend, in this instance of approximately 60 °, from its initial direction and then proceeds to move along a line close to the heading produced by the first bend. One characteristic of such a turn is its relatively slow angular velocity (see below). Such routine turns are made in a variety of directions and tend to have a relatively shallow turn angle for the initial bend, as shown for a set of seven turns made by a single larva (Fig. 3A). Fig. 3B illustrates all routine turns measured for a group of four larval fish. Other salient characteristics of routine turns are the relative lack of a counterbend after the initial turn and a relatively low-speed swim that sometimes follows the turn. These features of routine turns are all distinct from the escape turns described next.

A second class of turning behaviors consists of high-velocity turns associated with escape responses. In larval zebrafish, the escape responses are of the C-start variety, meaning that they are initiated by a very fast C-shaped bend (Fig. 4). These escape responses have been studied in detail (see, for example, Kimmel et al., 1980; Foreman and Eaton, 1993; Liu and Fetcho, 1999) and are shown here for comparison with routine turns. The escape response shown in Fig. 4 was elicited by a brief pulse of water puffed out of a pipette positioned near the head of the fish (highlighted in frame 1). In addition to the initial rapid bend (which is near maximal in frame 7), the escape response typically includes a large counterbend in the opposite direction, which reaches a maximum at frame 13 (asterisk). Fig. 5A shows a plot of the initial turn angles for six escape turns elicited from the fish used in Fig. 3A. The escape responses plotted here were elicited by pressure pulses directed at either the head (solid arrows) or tail (broken arrows). Fig. 5B shows all escape turns recorded from the same four fish depicted in Fig. 3B. In some instances, the turn angle exceeded 180 ° (open arrowheads). The escape response is typically

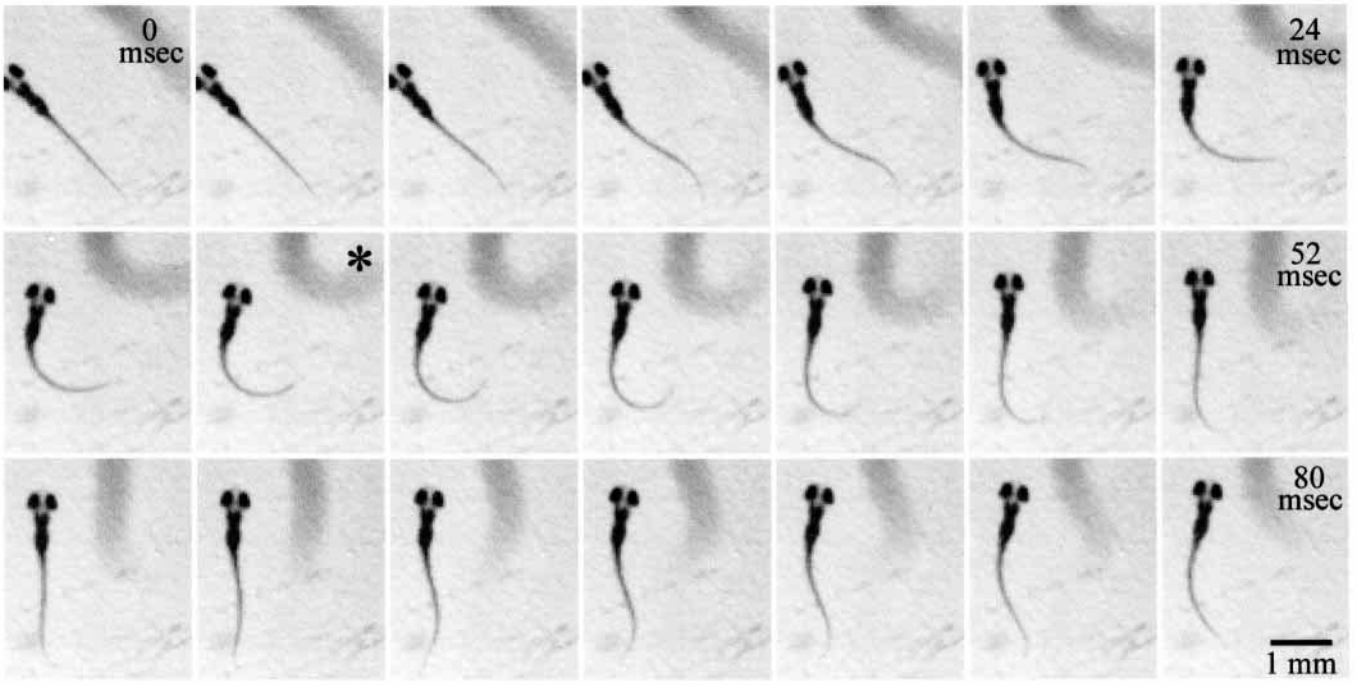

Fig. 2. Example of a routine turn. Images were collected at 500 frames s^{-1}, and every other frame is shown. Note the small angle and slow angular velocity of the turn, which begins in frame 2 and takes approximately 28 ms to reach a maximal change in heading (frame 9, asterisk). The initial bend to the right turns the fish close to its final orientation. There is only a slight subsequent counterbend in the opposite direction. The main turn of the larva is preceded by a very slight contralateral bend near the tip of the tail. This 'pre-bend' was not analyzed in this series of experiments. The kinematic measurements for this turn were: angular velocity 5.0 ° ms^{-1}, duration 28 ms, counterbend angle 33 °.

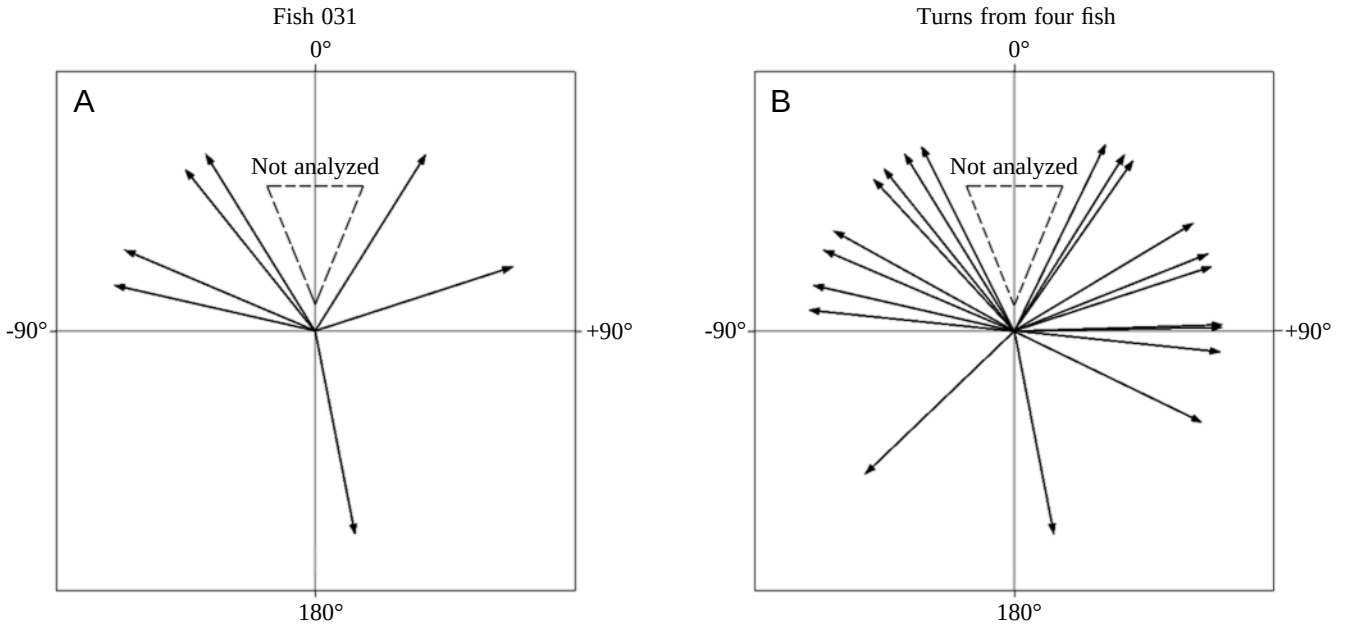

Fig. 3. Direction changes produced by routine turns. The change in direction produced by the initial turn is shown for seven routine turns recorded from one fish (A) and for a total of 20 routine turns recorded from four fish (B). The initial heading of the larva was normalized to 0°, and none of these turns resulted in a heading change greater than 180°. The gap about 0° reflects our criterion for selection of behaviors. Many swimming bouts begin with slight changes in heading, but ultimately result in movement along a more-or-less straight line. To exclude these behaviors from our analysis of routine turns, only those turns that exceeded approximately ±30° were used in the analysis. The two largest routine turns had relatively slow angular velocities (compared with escape turns; see below), measuring 6.7° ms^{-1} for the largest turn and 6.6° ms^{-1} for the second largest turn.

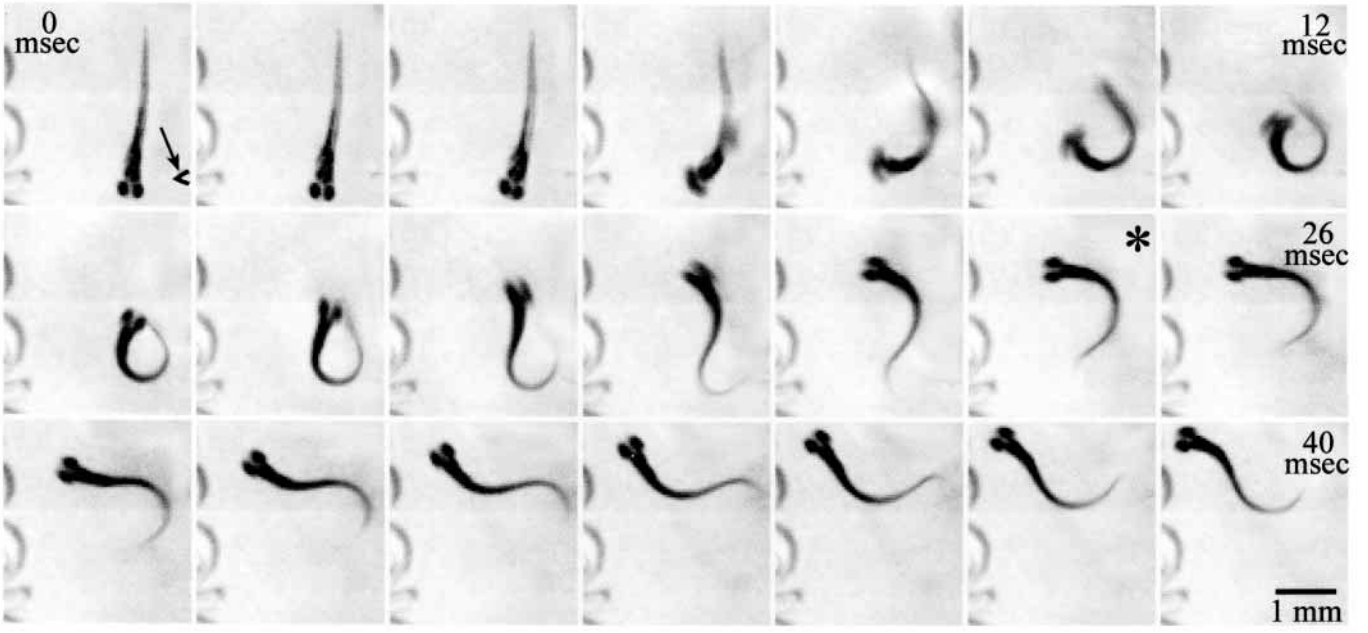

Fig. 4. Example of an escape turn. This turn was elicited by a puff of water from a micropipette (the arrow points to the highlighted tip of the pipette in frame 1). Images were collected at 500 frames s^{-1}, and every frame is shown. Note the high angular velocity of the initial bend, which takes approximately 12 ms to reach its maximum. Also note the large counterbend that approaches a C-shape in frame 13 (asterisk). In this and subsequent figures, the shadow of the fish (which can be seen in Fig. 2) was digitally removed for easier visualization. No pixels were altered that encompassed any part of the fish itself, and all analyses were performed on the raw images. The kinematic measurements for this turn were: angular velocity 20.7° ms^{-1}, duration 12 ms, counterbend angle 136°.

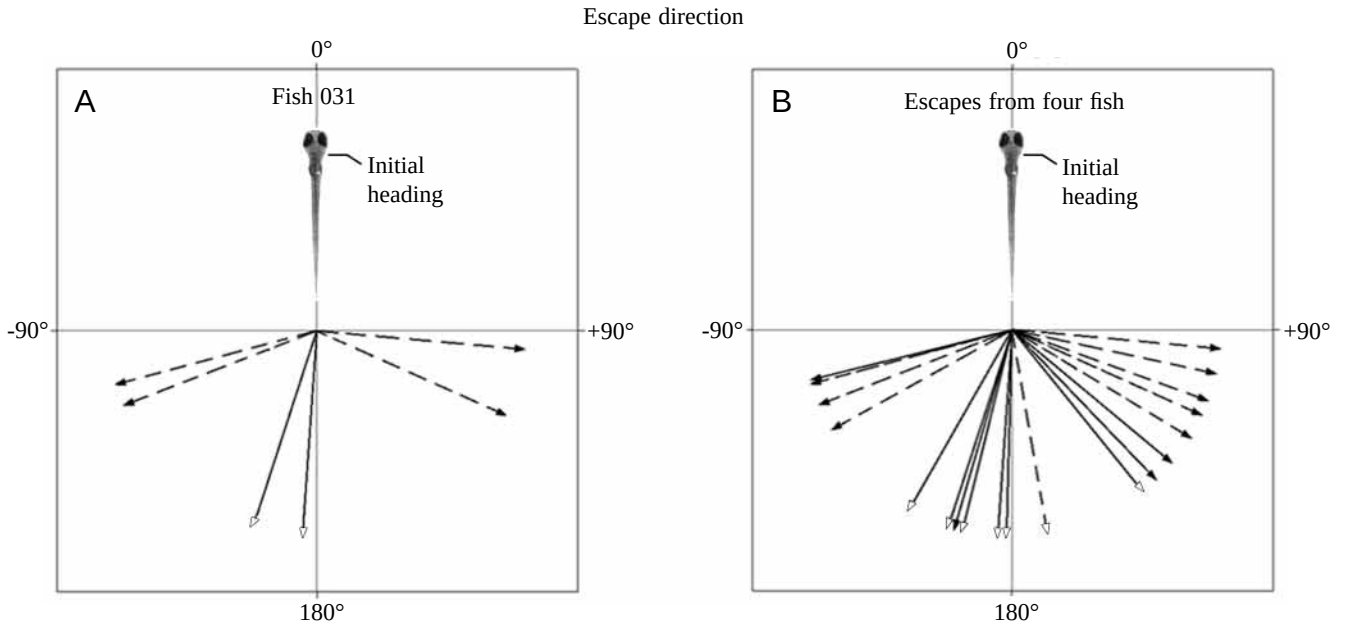

Fig. 5. Direction changes produced by escape turns. The change in direction produced by the initial bend of the escape is shown for six escapes recorded from one fish (A) and for a total of 19 escapes recorded from four fish (B). The initial heading of the larva was normalized to 0 ° (indicated by a silhouette). Note that the escape-turn angles range between 90 and 220 ° (angles greater than 180 ° are indicated by open arrowheads). Head-elicited escapes (solid arrows) tended to produce larger direction changes than escapes elicited by tail stimulation (broken arrows), in agreement with Eaton et al. (1984).

followed by a vigorous swimming episode, often referred to as a burst swim, as occurs in Fig. 4 following the counterbend. Such burst swims were not observed following routine turns.

An obvious difference between the two turning behaviors is that escape turns were elicited by a pressure pulse, whereas routine turns occurred ‘spontaneously’. Neither relationship, however, is absolute. ‘Spontaneous’ turns could, in principle, include *bona fide* escape responses to stimuli that were perceived by the fish but not apparent to us. Furthermore, while most pressure pulses elicit escape responses, not all do. Only short-latency, fast responses are believed to be *bona fide* escape responses produced by activation of the Mauthner cell (Eaton et al., 1984; Liu and Fetcho, 1999). A more rigorous approach is to categorize turns on the basis of angular velocity (Fig. 6A). While it turns out that the higher-velocity turns were pulse-elicited (shaded columns) and the slower velocity turns were ‘spontaneous’ (open columns), we did not use this as the basis for categorization. Instead, we chose an intermediate angular velocity (13 ° ms^{-1}) and classified turns as either routine (angular velocity below 13 ° ms^{-1}) or escape (angular velocity above 13 ° ms^{-1}). With this criterion, there was little overlap in the other turn variables measured. The initial bend of escape turns took 6–14 ms, whereas routine turns were of much longer duration, with most taking 24–34 ms (Fig. 6B). Routine turns were accompanied by minimal counterbending, in contrast to the large counterbend that accompanies escape turns (Fig. 6C). Moreover, inspection of the images (Figs 2, 4) shows that, in routine turns, only a small portion of the tail is bent during the counterbend, while in escape turns the counterbend involves essentially the entire body, which is suggestive of much larger contractile forces. These differences are behaviorally significant because, in escape turns, the counterbend can contribute both to propulsion and to the overall direction change of the fish (discussed by Foreman and Eaton, 1993).

Swimming patterns

Larval zebrafish often exhibit a relatively slow-speed pattern of swimming characterized by small bend angles and a locus of maximal bending (‘bend location’, see Materials and methods) located near the tail of the fish (Fig. 7). In the example shown in Fig. 7, the fish moved less than one-third of a body length in 88 ms. Such ‘slow’ swimming sometimes follows routine turns and is distinct from the faster pattern of swimming that typically follows escape responses. Fig. 8 shows the faster, more vigorous, ‘burst’ swimming pattern that is often associated with escapes. The burst swimming pattern exhibits larger bend angles and higher speeds than slow swimming, as well as a bend location that is closer to the mid-body of the fish. The fast swimming pattern was not exclusively associated with elicited escape behaviors. To characterize swimming, it was necessary to choose a criterion that would allow us to distinguish the two swimming patterns.

Slow swims appear, superficially, to consist of side-to-side movements of the tail, with little bending of the rostral half of the fish. Closer inspection, however, reveals an apparent rostral–caudal propagation of contractile waves. In comparison with burst swims, the greatest degree of bending occurs closer to the tail during slow swims. To quantify this, fish were examined at the time point during the swimming cycle when

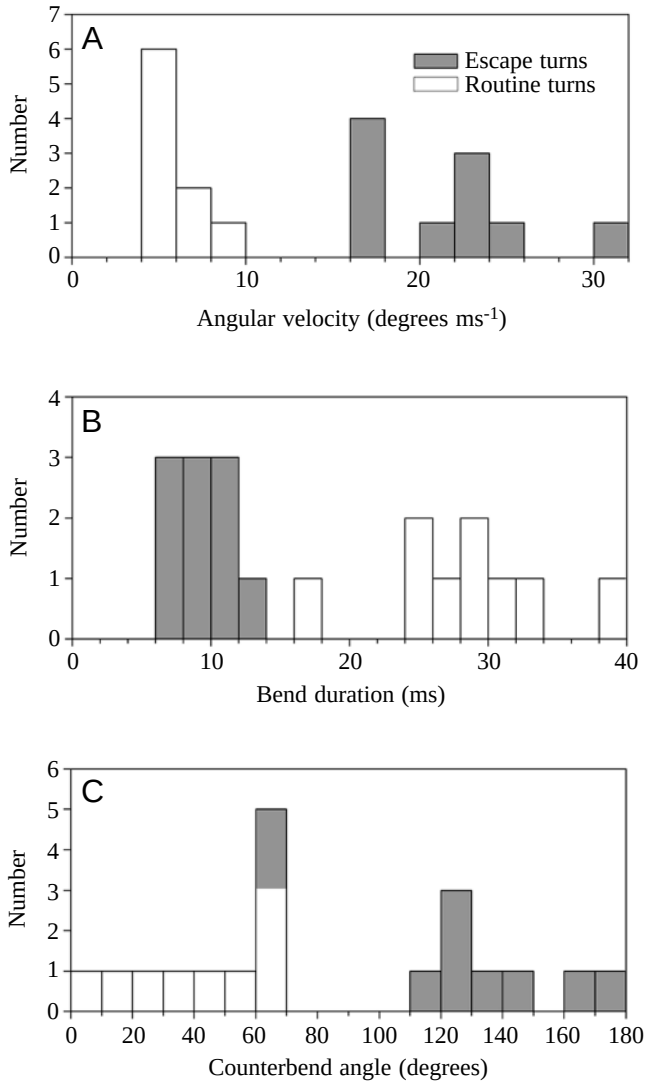

Fig. 6. Comparison of escape *versus* routine turns. (A) Histogram of the angular velocity of 19 turns. These turns were categorized as either escape turns (filled columns) or routine turns (open columns) on the basis of whether or not their angular velocity exceeded 13 ° ms^{-1}. On the basis of this classification, other aspects of the two turning behaviors were compared. The mean angular velocity of escape turns was 21.2±4.4 ° ms^{-1} (N=10) and that for routine turns was 6.0±1.0 ° ms^{-1} (N=9; means ± S.D.). (B) The duration of the bend (from rest until completion of the first bend) was, on average, almost three times longer for routine *versus* escape turns: 29.0±5.8 ° ms^{-1} (N=9) for routine turns and 10.4±2.1 ° ms^{-1} (N=10) for escape turns. (C) The counterbend angles were also distinct, with only two escape counterbends falling into the range of the much smaller routine counterbends: escape counterbends were 125.1±36.9 ° (N=10) and routine turn counterbends 42.4±20.8 ° (N=9) for routine turns. The differences in bend duration and in counterbend angle were highly significant (P<0.001).

the total curvature of the fish was maximal (see Materials and methods). This revealed that the fish is bent maximally about a fairly caudal point during slow swims, but during burst swims this bend location is closer to the mid-body. To categorize all the recorded swimming episodes, those with a caudal bend location (0.7 body lengths or more caudal) were classified as slow swims, while episodes with a more rostral bend location were classified as burst swims (Fig. 9A). On the basis of this criterion, we compared four other swimming variables. The degree of bending (mean bend amplitude), measured over three or more successive cycles of swimming, was greater for burst than for slow swims (Fig. 9B). More dramatic was the difference in swimming speed (Fig. 9C), which tended to be approximately 10 times faster for burst swims. Not surprisingly, the tail-beat frequency (Fig. 9D) was also faster for the burst swims. The last variable measured, yaw (the side-to-side movement of the head during swimming; Fig. 9E), was strikingly divergent between the two patterns of swimming. Burst swims had mean yaw angles ranging from 14 to 27 °, while slow swims had mean yaw angles of less than 3 °.

Prey capture

A more elaborate behavior exhibited by larval zebrafish within a few days after hatching is prey capture. Examples of predation upon *Paramecium* are shown in Fig. 10. This complex behavior appears to consist of simpler locomotor elements. A series of small 'routine-like' turns is apparently used by larval zebrafish to bring them in line with a swimming *Paramecium* (Fig. 10A; 100 ms per frame). Once the *Paramecium* is close to the larva, a brief swimming episode that appears to be similar to a slow swim is used to make a 'slow strike' to capture the *Paramecium* (Fig. 10B, 8 ms per frame; capture occurs immediately after the 1200 ms time point). In some instances, the larva appears to engulf the prey (termed 'ram' feeding). In these still images, the *Paramecium* are difficult to see because of their small size and low contrast and so they have been digitally enhanced, or highlighted. However, because of their motion, *Paramecium* are quite apparent when directly viewing movies of prey capture, and so their location is certain (see Materials and methods). Fig. 10A,B shows a 9-day-old fish, but at days 6 or 7, locomotor components to prey capture are not so well developed. Suction feeding at day 6 is clearly illustrated by the capture of a nearby *Paramecium* while the larva remains stationary (Fig. 10C). Note that the above ages refer to larvae maintained at room temperature; rearing at 27 °C would probably accelerate the development of prey-capture behaviors.

Discussion

Our goal was to characterize the locomotor repertoire of larval zebrafish with respect to its control by neurons in the brainstem. We have not attempted to address all aspects of locomotion. The use of pectoral fins and the maintenance of orientation with respect to gravity, for example, have not been analyzed. Nor can we comment on behaviors exhibited in a natural environment that might not be evident in a laboratory setting. Nonetheless, we have observed a significant behavioral repertoire. Larval zebrafish exhibit at least two distinct types

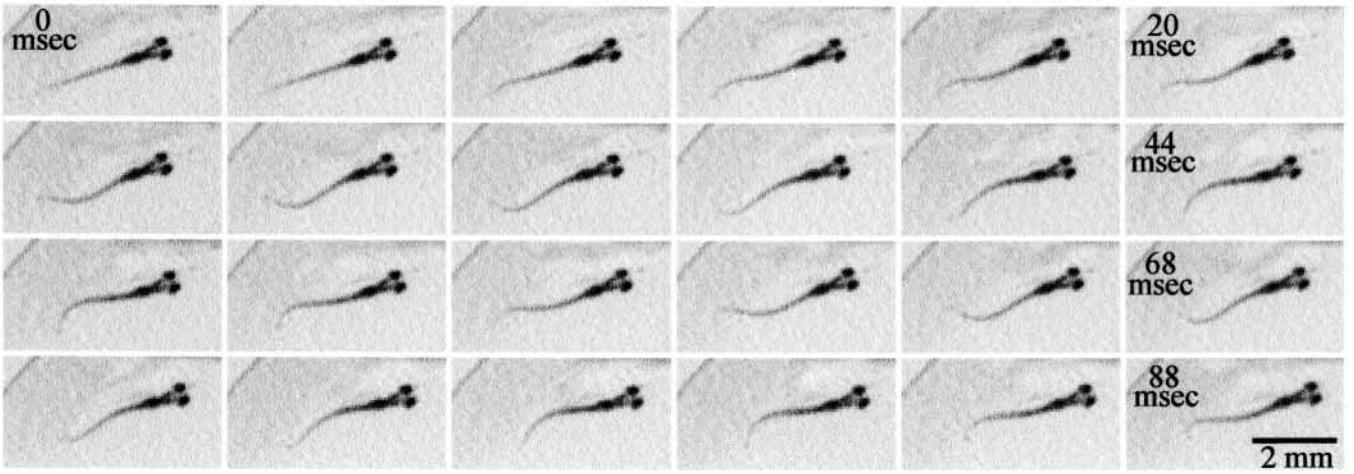

Fig. 7. Example of a slow swim. A spontaneous, relatively slow episode of swimming is shown. Images were collected at 500 frames s^{-1}, and every other frame is shown. This pattern of swimming appears to consist of rostral–caudal propagation of relatively mild bends, but there is only minimal lateral (side-to-side) movement of the head and minimal bending of the front half of the body. The tail-beat frequency (approximately two cycles in 80 ms) is low relative to the burst swimming pattern (see below). Note also the short distance traveled, less than 0.3 body lengths, during this set of images. All frames show exactly the same region of the dish. At the end of the swim, the direction of the fish is little changed from its initial heading. The kinematic measurements for this episode were: bend location 0.74 body lengths, mean bend amplitude 52.1 °, swimming speed 10.0 mm s^{-1}, tail-beat frequency 30.0 Hz, yaw 0.56 °.

of turning behavior, routine and escape turns, as well as two distinct patterns of swimming, burst and slow swimming. One possibility is that each behavioral variant is controlled by distinct, but possibly overlapping, sets of neurons in the brainstem. Before discussing this possibility, we should first consider whether control signals from the brainstem are needed for these behaviors. Studies of 'spinal' fish, in which a transection has been made at the spinal cord/brainstem juncture, are relevant to this issue.

Dogfish (*Scyliorhinus canicula*) show initially weak rhythmic activity after transection at the rostral end of the spinal cord. This activity strengthens over time and leads to continuous swimming (Mos et al., 1990), which might suggest that descending control signals are not required for swimming behaviors. Most teleost fish, however, respond differently. For example, after spinal transection just rostral to the dorsal fin, both goldfish and zebrafish are effectively paralysed below the transection (Bernstein and Gelderd, 1970; Van Raamsdonk et

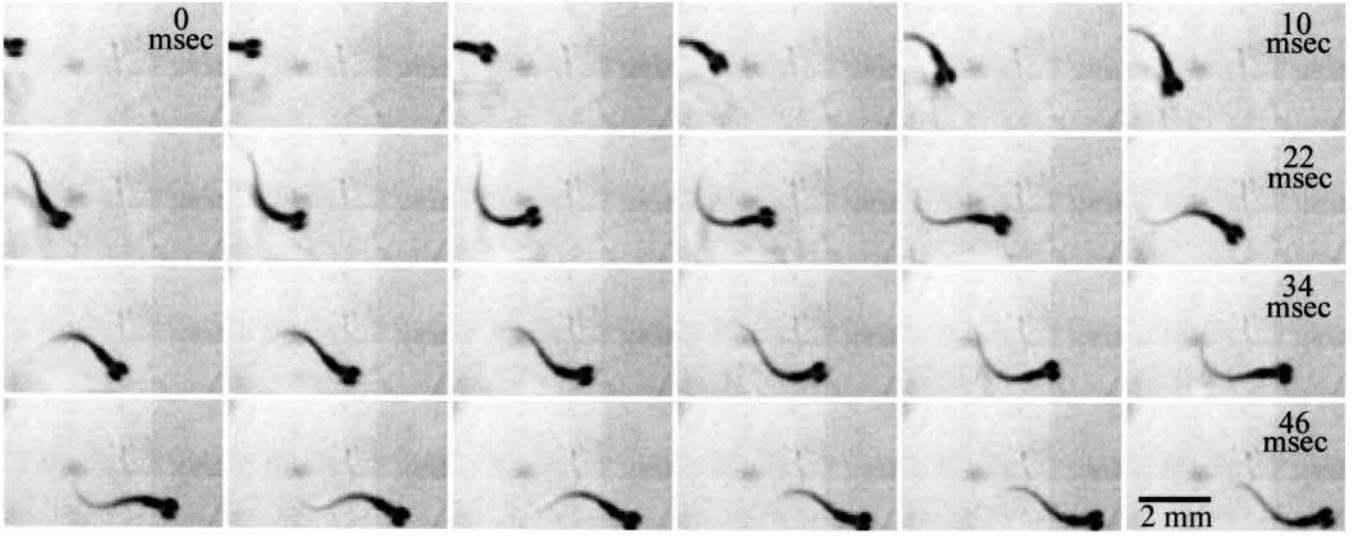

Fig. 8. Example of a burst swim. Images were collected at 500 frames s^{-1}, and all frames are shown. The size of this larva (3.5 mm) is nearly the same as that in Fig. 7, but the larva is shown here at a somewhat lower magnification so that several cycles of swimming can be seen. Note the more rostral 'bend location', the larger amplitude of bending and the much faster speed of this fish relative to that shown in Fig. 7. Also note the higher tail-beat frequency (a little under three cycles in 46 ms) and substantial lateral (side-to-side) movement of the head (termed 'yaw'). The kinematic measurements for this episode were: bend location 0.61 body lengths, mean bend amplitude 78.8 °, swimming speed 103.8 mm s^{-1}, tail-beat frequency 54.7 Hz, yaw 14.5 °.

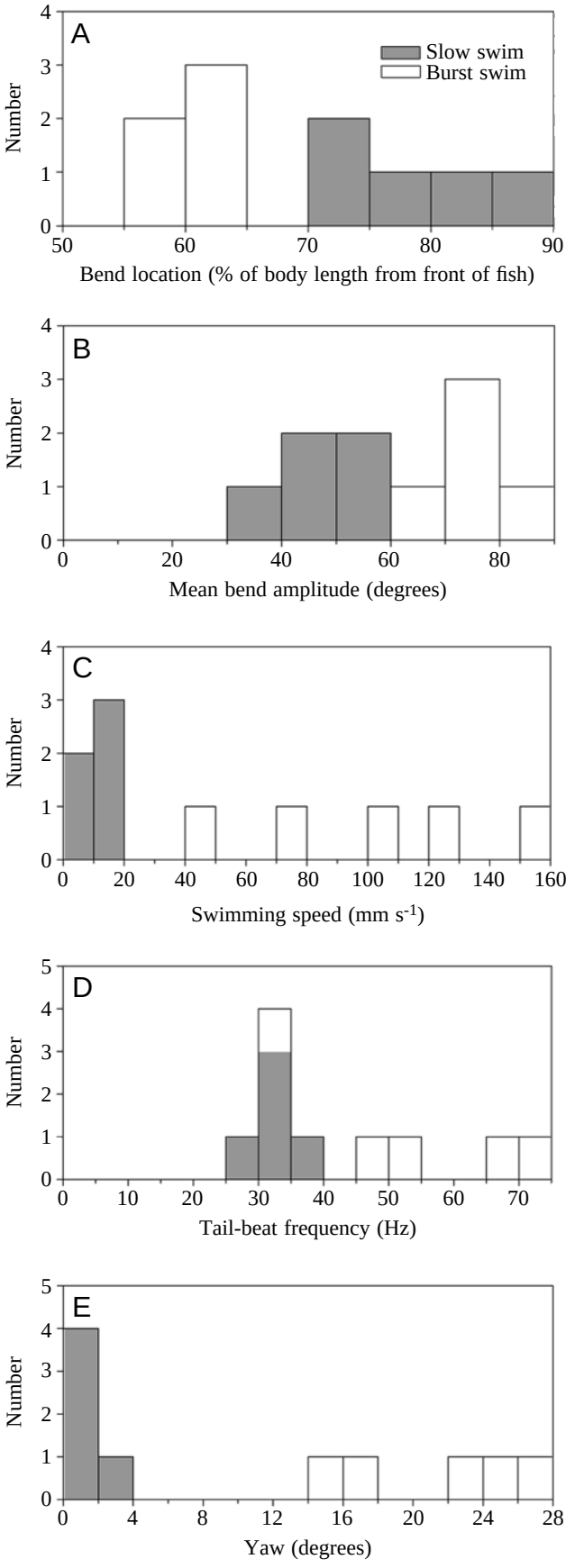

Fig. 9. Comparison of slow and burst swims. Bend location for different episodes of swimming was determined as shown in Fig. 1. (A) Episodes with bend locations of 0.7 body lengths or more caudal were classified as slow swims (filled columns), while those with more rostral bend loci were classified as burst swims (open columns). The histogram shows the number of swimming episodes recorded for a given bend location. The bend location of burst swims was 0.61±0.01 body lengths (N=5) and that for slow swims was 0.80±0.06 body lengths (N=5; means ± S.D.). On the basis of this classification, other aspects of the two swimming behaviors were compared. Significant differences were found for all four kinematic variables. (B) The mean bend amplitude was 75.4±6.7 °(N=5) for burst swims and 46.3±8.1 ° (N=5) for slow swims (P<0.01). (C) The mean swimming speed was 101.9±41.1 mm s^{-1} (N=5) for burst swims and 9.3±3.0 mm s^{-1} (N=5) for slow swims (P<0.01). (D) The mean tail-beat frequency was 56.6±15.8 Hz (N=5) for burst swims and 33.8±2.8 Hz (N=5) for slow swims (P<0.03). (E) The mean yaw was 21.3±5.2 ° (N=5) for burst swims and 1.4±0.8 ° (N=5) for slow swims (P<0.01).

al., 1998). In goldfish, it appears that swimming requires activity in a midbrain/mesencephalic locomotor region (MLR). Electrical stimulation of this region produces swimming, and the speed of swimming increases with increasing frequency and intensity of stimulation (Fetcho and Svoboda, 1993). Similar effects of MLR stimulation have been reported for carp (*Cyprinus carpio*) (Kashin et al., 1974) and more distantly related species such as the Atlantic stingray (*Dasyatis sabina*) (Livingston and Leonard, 1990) and lamprey (*Ichthyomyzon unicuspis*) (McClellan and Grillner, 1984). In general, acute spinal teleost fish do not exhibit undulatory swimming patterns or turning behaviors (Roberts and Mos, 1992). While central pattern generators (CPGs) reside in the spinal cord of many (probably all) vertebrate species, and are necessary for swimming (see, for example, Grillner and Wallen, 1985; Fetcho, 1992; Roberts et al., 1998), teleost fish are nearly immobile in the absence of descending control signals.

Swimming behaviors

Previous studies of larval swimming, examining ontogeny and temperature-dependence, have generally described a single pattern of swimming at specific developmental stages (Fuiman and Webb, 1988; Batty and Blaxter, 1992; but see Kimmel et al., 1974). Here, we report highly distinctive burst and slow swims. The kinematic differences between these swimming patterns (i.e. bend location, swimming speed and yaw) cannot be due to biomechanical differences between fish, nor to developmental stage, because both patterns were exhibited by individual fish within a short time interval. One possibility is that the more caudal bending seen in slow swims reflects activation of a more caudal grouping of motoneurons by caudally projecting reticulospinal neurons. This might seem simplistic, given the complex biomechanics involved in bending a fish (Wainwright, 1983), and indeed we expect there will be simultaneous activation of a number of myotomes for both types of swimming (Jayne and Lauder, 1996), but a precedent for the selective activation of posterior motoneurons

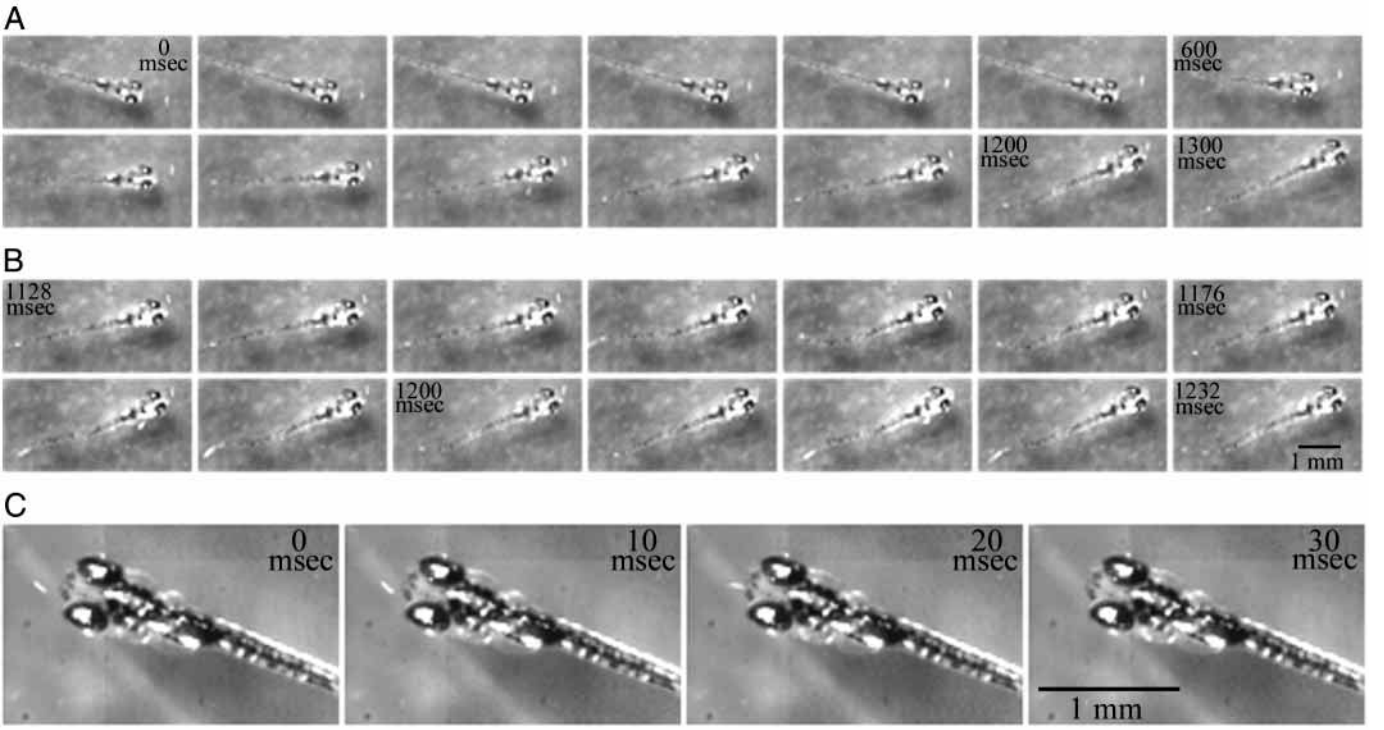

Fig. 10. Examples of prey capture. (A) To illustrate possible visual tracking of the prey, images are shown at 100 ms intervals. This 9-day-old larva makes several small 'routine-like' turns which brings it into alignment with the *Paramecium*, which is consumed shortly after the 1200 ms frame. (B) After apparently tracking the *Paramecium*, the larva, using its pectoral fins and a slow-swim-like pattern, propels itself towards and subsequently engulfs the *Paramecium*. The images in B are from the same feeding episode as in A, but are shown at 8 ms intervals. The *Paramecium* enters the larva's mouth at approximately 1208 ms. (C) A 6-day-old larva. The *Paramecium* moves abruptly towards and into the mouth of the larvae, demonstrating a suction-feeding mechanism, since the larva was stationary throughout the feeding episode.

exists in the eel *Anguilla rostrata*, in which anterior muscles are inactive during slow swimming (Gillis, 1998). In contrast, the nearly C-shaped contractions of the fish that occur during burst swims indicate a more synchronous activation of motoneurons along the rostral–caudal axis. It is not clear how this occurs, but it may be somewhat analogous to the escape behavior, in which the Mauthner cell initiates a nearly synchronous activation of motoneurons along the length of the fish (Nissanov and Eaton, 1989). A more traditional view is that swimming results from segment-to-segment progression of CPG activity along the rostral–caudal axis of the fish (Fetcho, 1992; Fetcho and Svoboda, 1993; Buchanan, 1996; but see Roberts et al., 1998). How descending control signals might interact with spinal CPGs to produce these very distinct patterns of swimming is not known. Regardless of the actual mechanism used, the spatiotemporal pattern of motoneuron activation must be different for the two types of swims, and the descending control signals must also be different.

Two distinct types of neural circuitry might be used to produce these swimming patterns. In dedicated circuitry, a specific set of neurons is used exclusively to control a specific behavior, whereas in distributed circuitry, control of the behavior is widely distributed throughout a group of neurons (Morton and Chiel, 1994). Because bouts of slow swimming can occur independently of other locomotor behaviors, it is tempting to speculate that they are controlled by a dedicated circuit. The differential innervation of red and white muscle by distinct populations of motoneurons (Westerfield et al., 1986; Fetcho, 1987; De Graaf et al., 1990; Roberts and Mos, 1992; also see Van Raamsdonk et al., 1996) is consistent with this idea. Furthermore, spinal swimming in dogfish appears to be mediated solely by red muscle (Mos et al., 1990), which suggests that the CPG controlling red-muscle-mediated (slow) swimming may be distinct from that controlling white-muscle-mediated (burst) swimming. These hypothetical CPGs could, in theory, be driven by distinct sets of hindbrain neurons dedicated to a specific swimming pattern. Our data do not, however, rule out the possibility that swimming is a continuum of behaviors, with slow and burst swimming representing two ends of a spectrum. Because burst swimming episodes invariably undergo a transition into a slower swimming pattern before the fish finally comes to a halt, it is possible that the control of swimming speed is distributed throughout a population of neurons. Swimming speed would be determined by the number and/or firing rate of active neurons. In this latter scheme, laser-ablation experiments would not selectively disrupt one type of swimming pattern, but instead would gradually degrade swimming performance in proportion to the number of hindbrain cells ablated.

Another possibility, based on the ability of the Mauthner cell

to reset the swimming rhythm (Svoboda and Fetcho, 1996) and the observation that burst swims commonly occur after escapes (Kimmel et al., 1974; Batty and Blaxter, 1992; Hale, 1996), is that burst swimming occurs primarily as a rebound effect produced by the spinal CPG as a result of its perturbation by the firing of the Mauthner cell. While this might conceivably occur in some instances, it is not the only means by which burst swims are initiated because we often observed burst swims that were not preceded by escape responses. More generally, many fish are capable of relatively sustained, white-muscle-mediated, high-speed swimming that appears to be independent of the escape response (Liu and Westerfield, 1988; Jayne and Lauder, 1994; Coughlin and Rome, 1996; Van Raamsdonk et al., 1998).

Turning behaviors

Turning behaviors are distinguished from swimming behaviors in two important respects. First, they are inherently asymmetric. This is apparent in the initial C-bend of escape behaviors (Fig. 4), and is also apparent during routine turns (Fig. 2), in which a single bend often occurs essentially in isolation from other substantial movements. The production of these asymmetric bends requires asymmetric muscle contraction and therefore asymmetric neural control. This is in contrast to bouts of straight-line swimming, in which a series of fairly symmetrical bends is observed, presumably involving alternating left–right activity in a spinal CPG. The second hallmark of a turn is that it is a unitary event, again well-illustrated by the routine turn that occurs in near isolation. The escape turn is more complex because it typically consists of an initial C-bend followed by a counterbend, both of which contribute substantially to the overall escape behavior (Foreman and Eaton, 1993). But, in both routine and escape turns, the initial bend is highly distinctive from the subsequent swimming (or turning) behavior, indicating a temporally precise neural control mechanism distinct from those producing swimming. This is best illustrated in the case of the Mauthner cell: it fires a single action potential in the initiation of an escape and is subsequently inhibited, making it the most temporally precise of the cells controlling turning behaviors (Zottoli, 1977; Faber et al., 1989; Eaton et al., 2000). While other reticulospinal neurons may fire multiple action potentials, regardless of the number of spikes fired, we would expect nerve cells controlling turning behaviors to have a phasic response preceding the turn.

Within the category of turning behaviors, we would expect further distinctions in the neural controls that produce routine *versus* escape turns. By firing just a single spike, the Mauthner cell produces a turn that is larger and faster than most routine turns (Nissanov et al., 1990), so the Mauthner cell cannot participate directly in the initiation of routine turns. The Mauthner cell homologues also contribute significantly to the escape because, in the absence of the Mauthner cell, escape turns of very large size and speed are still produced (Eaton et al., 1982, 2000; Liu and Fetcho, 1999). It seems unlikely, therefore, that the homologues of the Mauthner cell would participate in routine turns. A parsimonious hypothesis is that the Mauthner array is part of a circuit dedicated to the production of escape turns and does not participate in the production of routine turns. A further extension of this hypothesis derives from analysis of the escape counterbend. This counterbend appears to be controlled by neurons distinct from those generating the initial C-bend, since the two bend angles of the escape can be highly divergent (Eaton and Emberley, 1991). The cells proposed to generate this counterbend (referred to as A2 neurons) are hypothesized to be ipsilaterally projecting so as to produce a contraction ipsilateral to the stimulus (Foreman and Eaton, 1993; Eaton et al., 2000). Because the escape counterbends are larger and faster than routine turns, the A2 neurons might be part of a circuit dedicated to the production of the escape counterbend. Other evidence consistent with the dedicated circuit hypothesis is that routine turns are typically followed by a weak bout of slow swimming (Fig. 2), in contrast to the robust, burst swimming that follows escapes (Kimmel et al., 1974; Batty and Blaxter, 1992; Hale, 1996). Furthermore, firing of the Mauthner cell resets the swimming rhythm in goldfish (Svoboda and Fetcho, 1996), but in lamprey other hindbrain neurons only modulate the swimming rhythm (thereby producing a turn; McClellan and Hagevik, 1997), which might be expected of neurons controlling routine turns. These different effects on swimming behavior are consistent with the idea that distinct circuits control routine *versus* escape turns.

Recent observations complicate the dedicated circuit hypothesis. After laser-ablation of the Mauthner cell and its homologues, stimulus-evoked turns can be elicited that are quite substantial, approaching the size and speed of normal escape turns, although they occur at much longer latencies (Liu and Fetcho, 1999). These large, delayed (LD) turns are thus distinct from normal escape turns. They are also distinct from routine turns, because of their large size and speed. The neurons that produce these LD turns are obviously distinct from the cells of the Mauthner array, because those cells had been deleted. The LD-turn-producing neurons are also distinct from the A2/counterbend-producing neurons, because the counterbend occurs on the opposite side of the spinal cord from the LD turn. But are the LD-turn-producing neurons distinct from those producing routine turns? We hypothesize that the LD neurons project contralaterally because they are potentially acting in concert with the contralaterally projecting Mauthner array during normal escapes. However, only a small part of the descending neural pathway in larval zebrafish is composed of contralaterally projecting neurons, perhaps less than 25 cells in total, including the Mauthner array and approximately 10 T-reticular neurons. Are there enough of these contralaterally projecting neurons to provide control of both LD turns and routine turns, given the wide range of angles and angular velocities exhibited in both turn categories? If not, then ipsilaterally projecting neurons might be required to form a circuit dedicated to the control of routine turns. These arguments notwithstanding, the possibility that LD turns, routine turns and escape counterbends form a continuum of

turning behaviors, controlled by distributed circuitry, is not ruled out. Cellular-level, optical dissection of the neural control system seems necessary for understanding the type of neural architecture used to produce turning behaviors.

Prey capture

In addition to their swimming and turning repertoire, larval zebrafish are capable of more complex locomotor behaviors such as prey capture. Our observations show that prey capture consists of a series of small 'routine-like' turns followed by a 'slow-like' swim. This behavior is distinct from the C-start feeding pattern exhibited by clownfish (*Amphiprion perideraion*) larvae at a similar size and age (Coughlin, 1994). A more detailed analysis, however, is required to determine whether the locomotor components of larval zebrafish prey capture are equivalent to or merely similar to those of routine turns and slow swims. Even if the behaviors turn out to be kinematically equivalent, different sensory and appetitive inputs are presumably driving prey capture *versus* the more 'spontaneous' locomotor behaviors. So, even in such a case, it would still be possible for a distinct set of brainstem neurons to control prey capture. We also observed that zebrafish larvae are able to use suction feeding either after a 'slow-strike' approach to a *Paramecium* or when stationary. It also appears to be the case that, by 8 or 9 days post-fertilization, larvae can visually track the *Paramecium*. Taken together, these observations indicate that young teleost larvae are capable of integrating appetitive and visual information and are able to use this information to execute a well-coordinated and complex sequence of motor movements. It remains to be determined whether these larvae are capable of prey-search strategies such as those exhibited by recently hatched larval clownfish (Coughlin et al., 1992).

Concluding remarks

Our observations, together with earlier studies, demonstrate the considerable complexity of the zebrafish larva's locomotor repertoire. How will we deal with this complexity? One simplifying aspect of the larval zebrafish is that in the spinal cord there is a relatively small number of neuronal cell types, which are repeated in successive spinal segments (Bernhardt et al., 1990; Hale et al., 1999; Eisen, 1999; and see Fetcho and Faber, 1988). It is theoretically possible that these spinal neurons form a unified control system and that all descending control signals act through the same set of spinal circuitry. Simply by driving this spinal circuitry in differing ways, the various descending signals might produce different behaviors. Recent data, however, seem to contradict this hypothesis. Forbell et al. (1996) and Ritter and Fetcho (1998) have shown that different classes of spinal neurons are active during escapes *versus* swimming behaviors. While one interpretation of their data might be that turns and swims are controlled *via* different spinal circuits, we suggest an alternative hypothesis. Fast behaviors (escapes and burst swims) produce pronounced bending of the body, while slow behaviors (routine turns and slow swims) produce markedly less bending. If the salient characteristic is either the contractile force or the speed of propagation of rostral–caudal activity, we would predict that the descending signals triggering escapes/burst swims will activate different spinal elements from signals triggering routine turns/slow swims.

We thank Angela Lee and Naga Sankrithi for help with image analysis and rearing of *Paramecium*. We also thank Ethan Gahtan and two anonymous reviewers for helpful suggestions. This work was supported by NIH grant NS 37789.

References

Bass, A. H. and Baker, R. (1997). Phenotypic specification of hindbrain rhombomeres and the origins of rhythmic circuits in vertebrates. *Brain Behav. Evol.* **50** (Suppl. 1), 3–16.

Batty, R. S. and Blaxter, J. H. S. (1992). The effect of temperature on the burst swimming performance of fish larvae. *J. Exp. Biol.* **170**, 187–201.

Bernhardt, R. R., Chitnis, A. B., Lindamer, L. and Kuwada, J. Y. (1990). Identification of spinal neurons in the embryonic and larval zebrafish. *J. Comp. Neurol.* **302**, 603–616.

Bernstein, J. J. and Gelderd, J. B. (1970). Regeneration of the long spinal tracts in the goldfish. *Brain Res.* **20**, 33–38.

Brockerhoff, S. E., Hurley, J. B., Janssen-Bienhold, U., Neuhauss, S. C. F., Driever, W. and Dowling, J. E. (1995). A behavioral screen for isolating zebrafish mutants with visual system defects. *Proc. Natl. Acad. Sci. USA* **92**, 10545–10549.

Brodal, A. (1981). *Neurological Anatomy*, third edition. New York: Oxford University Press.

Buchanan, J. T. (1996). Lamprey spinal interneurons and their roles in swimming activity. *Brain Behav. Evol.* **48**, 287–296.

Coughlin, D. J. (1994). Suction prey capture by clownfish larvae (*Amphiprion perideraion*). *Copeia* **1**, 242–246.

Coughlin, D. J. and Rome, L. C. (1996). The roles of pink and red muscle in powering steady swimming in scup, *Stenotomus chrysops*. *Am. Zool.* **36**, 666–677.

Coughlin, D. J., Strickler, J. R. and Sanderson, B. (1992). Swimming and search behavior in clownfish, *Amphiprion perideraion*, larvae. *Anim. Behav.* **44**, 427–440.

De Graaf, F., Van Raamsdonk, W., Van Asselt, E. and Diegenbach, P. C. (1990). Identification of motoneurons in the spinal cord of the zebrafish *Brachydanio rerio* with special reference to motoneurons that innervate intermediate muscle fibers. *Anat. Embryol.* **182**, 93–102.

Domenici, P. and Blake, R. W. (1997). The kinematics and performance of fish fast-start swimming. *J. Exp. Biol.* **200**, 1165–1178.

Drost, M. R. and Van den Boogaart, J. G. M. (1986). The energetics of feeding strikes in larval carp *Cyprinus carpio*. *J. Fish Biol.* **29**, 371–380.

Eaton, R. C., Bombardieri, R. A. and Meyer, D. L. (1977). The Mauthner-initiated startle response in teleost fish. *J. Exp. Biol.* **66**, 65–81.

Eaton, R. C., DiDomenico, R. and Nissanov, J. (1991). Role of the Mauthner cell in sensorimotor integration by the brainstem escape network. *Brain Behav. Evol.* **37**, 272–285.

Eaton, R. C. and Emberley, D. S. (1991). How stimulus direction determines the trajectory of the Mauthner-initiated escape response in a teleost fish. *J. Exp. Biol.* **161**, 469–487.

Eaton, R. C., Lavender, W. A. and Wieland, C. M. (1981). Identification of Mauthner-initiated response patterns in goldfish: evidence from simultaneous cinematography and electrophysiology. *J. Comp. Physiol.* A **144**, 521–531.

Eaton, R. C., Lavender, W. A. and Wieland, C. M. (1982). Alternative neural pathways initiate fast-start responses following lesions of the Mauthner neuron in goldfish. *J. Comp. Physiol.* A **145**, 485–496.

Eaton, R. C., Lee, R. K. K. and Foreman, M. B. (2000). The Mauthner cell and other identified neurons of the brainstem escape network of fish. *Prog. Brain Res.* (in press).

Eaton, R. C., Nissanov, J. and Wieland, C. M. (1984). Differential activation of Mauthner and non-Mauthner startle circuits in the zebrafish: implications for functional substitution. *J. Comp. Physiol.* A **155**, 813–820.

Eisen, J. S. (1999). Patterning motoneurons in the vertebrate nervous system. *Trends Neurosci.* **22**, 321–326.

Faber, D. S., Fetcho, J. R. and Korn, H. (1989). Neuronal networks underlying the escape response in goldfish: general implications for motor control. *Ann. N.Y. Acad. Sci*. **563**, 11–33.

Fetcho, J. R. (1987). A review of the organization and evolution of motoneurons innervating the axial musculature of vertebrates. *Brain Res. Rev.* **12**, 243–280.

Fetcho, J. R. (1992). The spinal motor system in early vertebrates and some of its evolutionary changes. *Brain Behav. Evol.* **40**, 82–97.

Fetcho, J. R., Cox, K. and O'Malley, D. M. (1998). Monitoring activity in neuronal populations with single cell resolution in a behaving vertebrate. *Histochem. J.* **30**, 153–167.

Fetcho, J. R. and Faber, D. S. (1988). Identification of motoneurons and interneurons in the spinal network for escapes initiated by the Mauthner cell in goldfish. *J. Neurosci*. **8**, 4192–4213.

Fetcho, J. R. and Liu, K. S. (1999). Zebrafish as a model system for studying neuronal circuits and behavior. *Ann. N.Y. Acad. Sci.* **860**, 333–345.

Fetcho, J. R. and O'Malley, D. M. (1995). Visualization of active neural circuitry in the spinal cord of intact zebrafish. *J. Neurophysiol.* **73**, 399–406.

Fetcho, J. R. and O'Malley, D. M. (1997). Imaging neuronal networks in behaving animals. *Curr. Opin. Neurobiol.* **7**, 832–838.

Fetcho, J. R. and Svoboda, K. R. (1993). Fictive swimming elicited by electrical stimulation of the midbrain in goldfish. *J. Neurophysiol.* **70**, 765–780.

Forbell, E., Cambronero, N. F., Ross, S. and Fetcho, J. R. (1996). Spinal interneurons involved in the escape behavior identified by *in vivo* calcium imaging in zebrafish. *Soc. Neurosci. Abstr.* **22**, 1374.

Foreman, M. B. and Eaton, R. C. (1993). The direction change concept for reticulospinal control of goldfish escape. *J. Neurosci.* **13**, 4101–4113.

Fraser, S., Keynes, R. and Lumsden, A. (1990). Segmentation in the chick embryo hindbrain is defined by cell lineage restrictions. *Nature* **344**, 431–435.

Fuiman, L. A. and Webb, P. W. (1988). Ontogeny of routine swimming activity and performance in zebra danios (Teleostei: Cyprinidae). *Anim. Behav.* **36**, 250–261.

Gillis, G. B. (1998). Neuromuscular control of anguilliform locomotion: patterns of swimming in red and white muscle activity during swimming in the American eel *Anguilla rostrata*. *J. Exp. Biol.* **201**, 3245–3256.

Grillner, S. and Wallen, P. (1985). Central pattern generators for locomotion, with special reference to vertebrates. *Annu. Rev. Neurosci.* **8**, 233–261.

Guthrie, S. (1995). The status of the neural segment. *Trends Neurosci.* **18**, 74–79.

Hale, M. E. (1996). The development of fast-start performance in fishes: Escape kinematics of the chinook salmon (*Oncorhynchus tshawytscha*). *Am. Zool.* **36**, 695–709.

Hale, M. E., Ritter, D., Bhatt, D., Higashijima, S., Okamoto, H. and Fetcho, J. R. (1999). A confocal study of spinal interneurons in larval zebrafish. *Soc. Neurosci. Abstr.* **25**, 1909.

Harper, D. G. and Blake, R. W. (1989). On the error involved in high-speed film when used to evaluate maximum accelerations of fish. *Can. J. Zool.* **67**, 1929–1936.

Jayne, B. C. and Lauder, G. V. (1994). How swimming fish use slow and fast muscle fibers: implications for models of vertebrate muscle recruitment. *J. Comp. Physiol.* A **175**, 123–131.

Jayne, B. C. and Lauder, G. V. (1996). New data on axial locomotion in fishes: how speed affects diversity of kinematics and motor patterns. *Am. Zool.* **36**, 642–655.

Kashin, S. M., Feldman, A. G. and Orlovsky, G. N. (1974). Locomotion of fish evoked by electrical stimulation of the brain. *Brain Res.* **82**, 41–47.

Kimmel, C. B., Eaton, R. C. and Powell, S. L. (1980). Decreased fast-start performance of zebrafish larvae lacking Mauthner neurons. *J. Comp. Physiol.* A **140**, 343–350.

Kimmel, C. B., Metcalfe, W. K. and Schabtach, E. (1985). T-reticular interneurons: a class of serially repeating cells in the zebrafish hindbrain. *J. Comp. Neurol.* **233**, 365–376.

Kimmel, C. B., Patterson, J. and Kimmel, R. O. (1974). The development and behavioral characteristics of the startle response in the zebrafish. *Devl. Psychobiol.* **7**, 47–60.

Lee, R. K. K. and Eaton, R. C. (1991). Identifiable reticulospinal neurons of the adult zebrafish, *Brachydanio rerio*. *J. Comp. Neurol.* **304**, 34–52.

Lee, R. K. K., Eaton, R. C. and Zottoli, S. J. (1993). Segmental arrangement of reticulospinal neurons in the goldfish hindbrain. *J. Comp. Neurol.* **329**, 539–556.

Liu, D. W. and Westerfield, M. (1988). Function of identified motoneurones and co-ordination of primary and secondary motor systems during zebrafish swimming. *J. Physiol., Lond.* **403**, 73–89.

Liu, K. S. and Fetcho, J. R. (1999). Laser ablations reveal functional relationships of segmental hindbrain neurons in zebrafish. *Neuron* **23**, 325–335.

Livingston, C. A. and Leonard, R. B. (1990). Locomotion evoked by stimulation of the brainstem in the Atlantic stingray, *Dasyatis sabina*. *J. Neurosci.* **10**, 194–204.

McClellan, A. D. and Grillner, S. (1984). Activation of 'fictive swimming' by electrical microstimulation of the lamprey central nervous system. *Brain Res.* **300**, 357–361.

McClellan, A. D. and Hagevik, A. (1997). Descending control of turning locomotor activity in larval lamprey: neurophysiology and computer modeling. *J. Neurophysiol.* **78**, 214–228.

Metcalfe, W. K., Mendelson, B. and Kimmel, C. B. (1986). Segmental homologies among reticulospinal neurons in the hindbrain of the zebrafish larva. *J. Comp. Neurol.* **251**, 147–159.

Morton, D. W. and Chiel, H. J. (1994). Neural architectures for adaptive behavior. *Trends Neurosci.* **17**, 413–420.

Mos, W., Roberts, B. L. and Williamson, R. (1990). Activity patterns of motoneurons in the spinal dogfish in relation to changing fictive locomotion. *Phil. Trans. R. Soc. Lond. B* **330**, 329–339.

Müller, U. K., Stamhuis, E. J. and Videler, J. J. (2000). Hydrodynamics of unsteady fish swimming and the effects of body size: comparing the flow fields of fish larvae and adults. *J. Exp. Biol.* **203**, 193–206.

Nissanov, J. and Eaton, R. C. (1989). Reticulospinal control of rapid escape turning maneuvers in fishes. *Am. Zool.* **29**, 103–121.

Nissanov, J., Eaton, R. C. and DiDomenico, R. (1990). The motor output of the Mauthner cell, a reticulospinal command neuron. *Brain Res.* **517**, 88–98.

O'Malley, D. M., Kao, Y.-H. and Fetcho, J. R. (1996). Imaging the functional organization of zebrafish hindbrain segments. *Neuron* **17**, 1145–1155.

Nicolson, T., Rüsch, A., Friedrich, R. W., Granato, M., Ruppersberg, J. P. and Nüsslein-Volhard, C. (1998). Genetic analysis of vertebrate sensory hair cell mechanosensation: the zebrafish circler mutants. *Neuron* **20**, 271–283.

Prasada Rao, P. D., Jadhao, A. G. and Sharma, S. C. (1987). Descending projection neurons to the spinal cord of the goldfish, *Carassius auratus*. *J. Comp. Neurol.* **265**, 96–108.

Ritter, D. and Fetcho, J. R. (1998). Confocal calcium imaging of spinal interneurons during swimming in larval zebrafish. *Soc. Neurosci. Abstr.* **24**, 1667.

Roberts, A., Soffe, S. R., Wolf, E. S., Yoshida, M. and Zhao, F.-Y. (1998). Central circuits controlling locomotion in young frog tadpoles. *Ann. N.Y. Acad. Sci.* **860**, 19–34.

Roberts, B. L. and Mos, W. (1992). Neural circuits for speed change in swimming fish. In *Neurobiology of Motor Programme Selection: New Approaches to the Study of Behavioural Choice* (ed. L. Kien, C. R. McCrohan and W. Winlow), pp. 123–146. Oxford, New York: Pergamon Press.

Saint-Amant, L. and Drapeau, P. (1998). Time course of the development of motor behaviors in the zebrafish embryo. *J. Neurobiol.* **37**, 622–632.

Siegel, J. M. and Tomaszewski, K. S. (1983). Behavioral organization of reticular formation: studies in the unrestrained cat. I. Cells related to axial, limb, eye and other movements. *J. Neurophysiol.* **50**, 696–716.

Spierts, I. L. Y. and Van Leeuwen, J. L. (1999). Kinematics and muscle dynamics of C- and S-starts of carp (*Cyprinus carpio* L.). *J. Exp. Biol.* **202**, 393–406.

Svoboda, K. R. and Fetcho, J. R. (1996). Interactions between the neural networks for escape and swimming in goldfish. *J. Neurosci.* **16**, 843–852.

Van Raamsdonk, W., Bosch, T. J., Smit-Onel, M. J. and Maslam, S. (1996). Organization of the zebrafish spinal cord: distribution of motoneuron dendrites and 5-HT containing cells. *Eur. J. Morph.* **34**, 65–67.

Van Raamsdonk, W., Maslam, S., de Jong, D. H., Smit-Onel, M. J. and Velzing, E. (1998). Long term effects of spinal cord transection in zebrafish: swimming performances and metabolic properties of the neuromuscular system. *Acta Histochem.* **100**, 117–131.

Wainwright, S. A. (1983). To bend a fish. In *Fish Biomechanics* (ed. P. W. Webb and D. Weihs), pp. 68–91. New York: Praeger Publishers.

Wardle, C. S., Videler, J. J. and Altringham, J. D. (1995). Tuning in to fish swimming waves: body form, swimming mode and muscle function. *J. Exp. Biol.* **198**, 1629–1636.

Westerfield, M. (1995). *The Zebrafish Book: A Guide for the Laboratory Use of Zebrafish (*Brachydanio rerio*)*. Third edition. Eugene, OR: University of Oregon Press.

Westerfield, M., McMurray, J. V. and Eisen, J. S. (1986). Identified motoneurons and their innervation of axial muscles in the zebrafish. *J. Neurosci.* **6**, 2267–2277.

Zottoli, S. J. (1977). Correlation of the startle reflex and Mauthner cell auditory responses in unrestrained goldfish. *J. Exp. Biol.* **66**, 243–254.